



# AirCargoChallenge 2022

# Technical Report

Team #22

ICARUS Polito



**ICARUS**  
**Polito**

# Contents

<b>Introduction</b>	<b>2</b>
<b>Project Management</b>	<b>3</b>
About us . . . . .	3
Budget and time schedule . . . . .	3
Organization . . . . .	4
<b>Flight dynamics</b>	<b>6</b>
Preliminary sizing . . . . .	6
Propulsion . . . . .	6
Flight envelope . . . . .	6
Tail sizing and stability . . . . .	7
Controls . . . . .	8
<b>Aerodynamics design</b>	<b>9</b>
Main wing . . . . .	9
Flap . . . . .	10
Winglets . . . . .	11
Full model simulations . . . . .	13
<b>Structural design</b>	<b>14</b>
Fuselage . . . . .	14
Wing . . . . .	15
Tail . . . . .	16
Landing Gear . . . . .	19
<b>Manufacturing</b>	<b>21</b>
Moulds . . . . .	21
Lamination . . . . .	21
<b>Payload Prediction</b>	<b>23</b>
<b>Outlook</b>	<b>24</b>
<b>Drawings</b>	<b>25</b>

# Introduction

ICARUS Team was founded in 2015 by 10 Air Cargo Challenge enthusiasts filled with dedication and passion for aerospace. Our team's ACC division participated in 2017 and 2019 editions of the challenge, achieving respectively 9th and 6th place. For 2022 we will take part in the competition with our brand new aircraft model, ICHOR. Since regulations for this year prescribe a payload composed by "small blood bags", the name we chose was inspired by

*ιχωρ*

the ethereal fluid that in Greek mythology composes the blood of Gods and Immortals.

# Project Management

## About us

The ACC division of our team consists of 17 students coming mainly from Aerospace and Mechanical Engineering BSc and MSc degree programmes held at Politecnico di Torino. We all have different backgrounds and our geographical breakdown reflects almost every corner of our beautiful country. The spirit of our team is naturally prone to diversity and inclusion, as we look forward to welcome on board more foreign students and to get a more balanced gender distribution in our future growth. If you are curious about the faces behind our projects, please visit <https://icarus.polito.it/i-volti-del-team/>.

## Time schedule and Budget

Preparation for ACC 2022 ideally started with our first participation to the competition in 2017. Since then, the continuous improvement in design, technology and organization has represented the guide throughout our activities. Much of the time spent before this year's regulations were published had been dedicated to capitalizing on knowledge and skills already acquired: that's why we chose to start the timeline (fig.1) with the "dummy project", a simulation of the competition based on a revised ACC regulation. This is our usual way to share experience with new members and to get prepared to the upcoming competition. The activities specifically dedicated to ACC 2022 started with the publication of regulations in August 2020 and are set to continue until June 2022, following the schedule in fig.1. We are planning to perform the first flight well in advance in order to validate the underlying design and introduce improvements as necessary.

	2019		2020				2021				2022				
	Sep	Dec	Jan	Aug	Oct	Dec	Jan	Mar	Apr	Sep	Dec	Jan	Apr	May	Jun
<b>Research / Gap year dummy projects</b>															
<b>Conceptual design</b>															
<b>Preliminary design</b>															
<b>Detailed design</b>															
<b>Construction</b>															
<b>First Flight (forecast)</b>															

Figure 1: Timeline

Our budget for ACC 2022 sums up to approximately 14580€ including travel ex-

penses, participation fees and operating costs. All the financial figures are an estimation and include some expenses in common with the other 2 divisions in our team (DART, RA) which we are not able to decouple. Funding is integrally provided by Politecnico di Torino, while additional support comes from our sponsors ALTAIR and SIEMENS who supply us fundamental software for FEM and CFD.

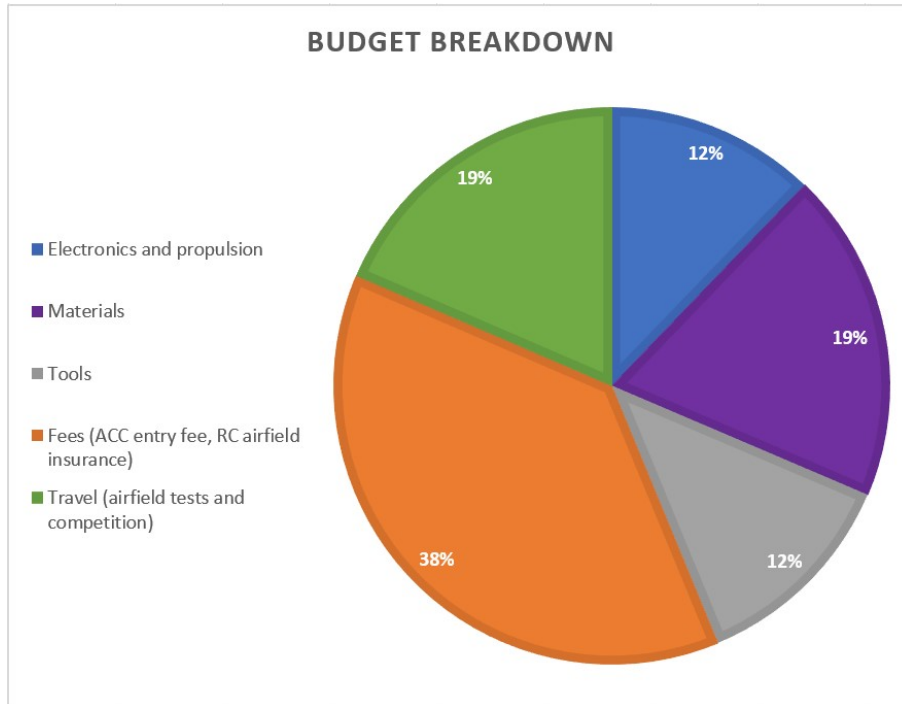


Figure 2: Budget for ACC 2022

## Organization

### Design phase

Conceptual and Preliminary Design phases took place in the middle of COVID-19 pandemic, so we were forced to interact only remotely. We adopted the well-run division of labor consisting in the 3 areas of Aerodynamics, Flight Mechanics and Structures, each area being composed of an almost equal number of members (3 or 4 people) and coordinated by an Area Head. During a typical week, each area worked mostly alone on its domain, then reported on achievements on the day appointed for the general meeting held on Zoom/GMeet. Much was performed individually, so we put in place a systematical written reporting activity in order for others and future members to benefit from each one's work. Overall coordination was ensured by a single Project Manager, which was also appointed as Head of Flight Dynamics. Some changes took place by September 2021 once every team member had moved back to Turin and the Preliminary Design phase had left room to Detailed Design. We kept the same division but benefited from the possibility to organize general meetings on Politecnico's premises, while area meetings were held either virtually or

at Toolbox Coworking Torino, a co-working space where we shared an office with 3 other student teams. The key change definitely was the lifting of heavy restrictions, which finally allowed us to meet in person for the first time increasing the bond and alchemy between us.

## **Construction**

Except for 4 members physically located in Turin when the pandemic hit, many others weren't able to work on construction until late 2021. Starting from that moment we organized the activities in our laboratory basing on the concept of Work-Packages (WPs), small groups comprising 2 to 4 people who were in charge of the construction of a given component or tool. 2 special WPs were introduced at this stage, namely CAD and Additive, given the increased need of developing ultimate geometries or components and tools in a limited time frame. Members with modeling experience and the Project Manager ensured the coordination between WPs, summarizing and dividing the activities with the aid of Trello boards. General live meetings were maintained in order to exchange updates and manage tasks effectively.

# Flight dynamics

## Preliminary sizing

Given the change in regulations, we needed a baseline to know which choices would be the best for our design. We developed a MATLAB script that generated a long list of "candidate planes" within the regulations, evaluated their performance based on the new scoring system, and provided an estimate of the best candidate to kickstart the design process.

Thanks to an iterative process with the help of the Aerodynamics section of the team, we obtained a first sizing of the aircraft. Later revisions, helped by CFD analysis, refined the design.

## Propulsion

The new regulations require the use of a different motor and propeller from ACC19, for which we did not have any experimental data. For this reason we researched publicly available databases for some performance data, but even though this was helpful for our evaluation, the motor-propeller match that we were going to use was not available. In previous years we were able to use the wind tunnel of our university to make real measurements, but with the COVID situation this was not possible.

Therefore, we used the data in our possession to build our own model by interpolating the performance of similar propellers and the datasheet of the motor. By intersecting the torque of the motor and the resistance of the propeller, various equilibrium points were found, allowing us to draw the working line of this assembly at various speeds (Fig. 3)

The equation for the working line (approximated to a parabola) is:

$$T = -0.0037 \cdot V^2 - 0.3683 \cdot V + 16.9020$$

Using our preliminary design, we determined that the cruise speed should be approximately 25 m/s.

## Flight envelope

**Takeoff** Using a MATLAB script we analyzed the takeoff run by evaluating the forces at play. We initially used some rough estimates of drag and mass, obtained from XFLR5 and previous experience with building methods, later refining them with CFD data and the mass of built parts. We have a high confidence on managing

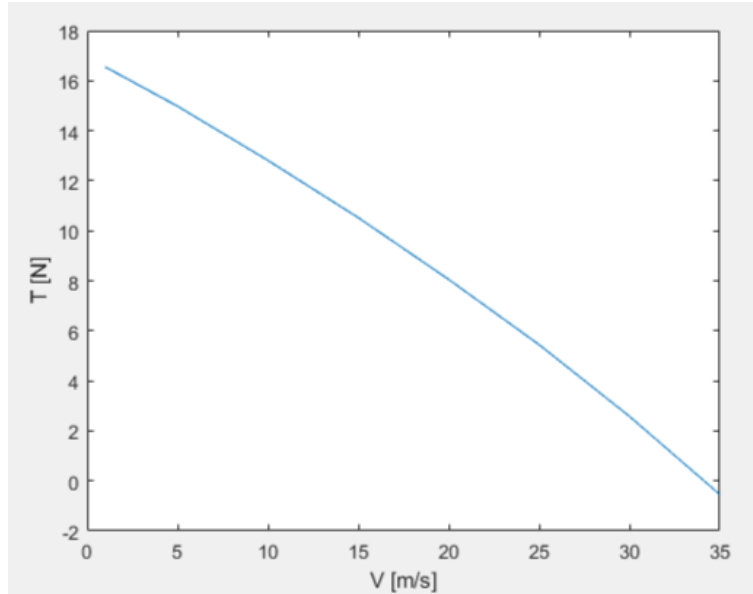


Figure 3: Thrust-Velocity curve resulting from motor-propeller matching

to take off in less than 60 meters, but more detailed estimates (accounting for flaps) and real life testing are required to know if the 40 meters target is achievable.

**Mission profile** To help us plan a strategy for flight and evaluate things such as bank angles, area limits, and battery usage, we simulated the whole mission profile in MATLAB using realistic flight performance parameters. We generated flight path visualizations (Fig. 4) that also helped the pilots get to know the mission profile and get a more intuitive understanding of the flight.

## Tail sizing and stability

The main constraint for the horizontal stabiliser sizing was the rhombus shape that the aircraft had to fit into. A MATLAB script was used to iterate over the possible tails that made the aircraft stable, trying to minimize the wetted surface. The Aspect Ratio of the horizontal stabilizer was monitored to take into account responsiveness and aerodynamic efficiency. The stabilizers that were compatible with the requirements were then further tested in XFLR5, taking into account the airfoil shape and verifying the static margin and the slope of the  $C_M - \alpha$  curve.

The final horizontal stabilizer has a span of 0.5 m, a root chord of 0.135 m and a trapezoidal shape. We chose a NACA 0010 airfoil, since we did not need too much vertical space for the servo, which is going to be mounted in the fin. The stabilizer is tilted by  $-1.5^\circ$ .

We also checked the dynamic stability of the aircraft, verifying that all the modes are dampened.

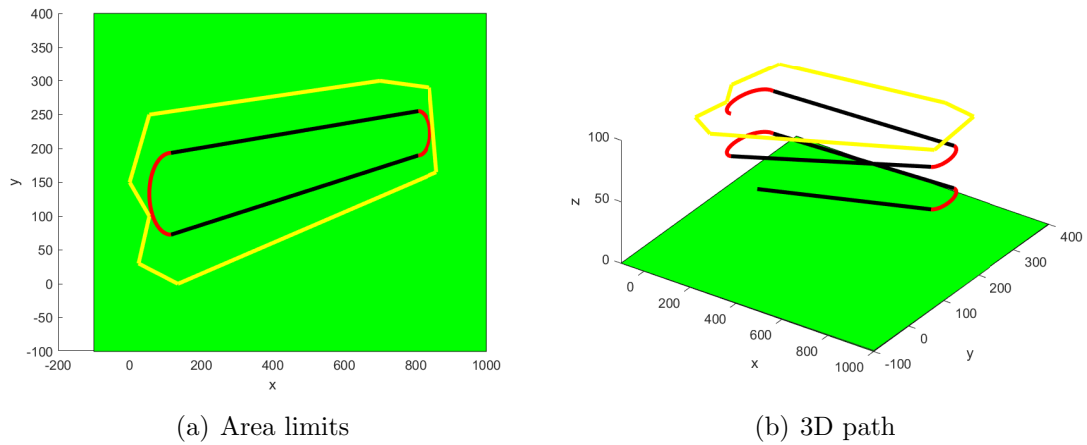


Figure 4: Flight path

## Controls

Using XFLR5 we simulated the wing with different aileron deflections and sizes, determining the rolling moment of the wing. We then computed the resulting rolling rates to compare them with the mission profile. A compromise was reached between the span of the aileron and flap span, choosing a configuration which was compatible both with control and aerodynamics needs.

The aileron covers 40% of the wing span and has a chord of 25% the wing's one, and deflects to a maximum of  $\pm 20^\circ$ .

# Aerodynamics design

## Main wing

The main wing was, together with the fuselage, the first part of the airplane that we began designing. The first phase was fairly iterative, as the variables at play were many and the geometry had to be chosen from scratch: wingspan, aspect ratio, airfoil, taper ratio, dihedral.

One of the first decisions we made was to have a wingspan just wide enough that each semi-wing could be stored in the transportation box without additional sectioning. This also implied that the shape of the planform would be a simple trapezoid, as making a more complex wing shape without sections was deemed too complicated for our manufacturing techniques.

Efficiency being crucial, we opted for the maximum aspect ratio that we could accommodate: the rhombus angles were chosen, together with the flight dynamics team, to be  $60.2^\circ$  and  $119.8^\circ$  respectively. The wing is placed exactly on the main diagonal, in order to extract the maximum wingspan possible.

The total mass at takeoff with maximum payload was estimated to be around 4.5 Kg, therefore the preliminary dimensions for the main wing were calculated as follows:

- Wingspan:  $b = 2.37m$ ;
- Root chord:  $c_r = 0.22m$ ;
- Tip chord:  $c_t = 0.1m$ ;
- Surface area:  $S = 0.3792 m^2$ ;
- Aspect ratio:  $AR = 14.88$ ;
- Taper ratio:  $\lambda = 0.455$ ;
- Target  $C_L$  at  $\alpha = 0^\circ$ :  $C_{L(target)} = 0.31$ ;

Different airfoils were first tested in XFLR5 and later in STAR CCM+ to gather data on the different aerodynamic coefficients and properties.

The airfoil we chose in the end is the AH 79-100 A and 2D CFD simulations provided results listed in Table 1. The airfoil stalls at around  $\alpha = 14^\circ$ .

Having chosen the main geometry of the wing and the airfoil, the next step was to simulate the 3D properties of the isolated wing and decide whether a dihedral

	$\alpha = -2^\circ$	$\alpha = 0^\circ$	$\alpha = 3^\circ$	$\alpha = 5^\circ$
$C_l$	0,2182	0,4389	0,7531	0,9535
$C_d$	0,0151	0,0153	0,017	0,0192
$E$	14,4503	28,6863	44,3000	49,6615
$C_m$	-0,1059	-0,1068	-0,1049	-0,1025

Table 1: Airfoil simulation results

	$\alpha = -1^\circ$	$\alpha = -0.5^\circ$	$\alpha = 0^\circ$	$\alpha = 0.25^\circ$	$\alpha = 0.5^\circ$	$\alpha = 1^\circ$
$L$	37.997	44.547	51,405	54,313	57.535	64.036
$D$	2.682	2.768	2.870	2,934	2.985	3.141
$E$	14,170	16.092	17.914	18.512	19.274	20.387
$C_L$	0.270	0.317	0.366	0.386	0.409	0.455
$C_D$	0.019	0.020	0.020	0.021	0.021	0.022

Table 2: Isolated wing simulation results

could be useful for lateral stability. Simulations were carried out again both in XFLR5 and STAR CCM+ and a dihedral of  $3^\circ$  positive was chosen. Due to structural requirements and limitations, the wing dihedral does not start from the fuselage axis ( $y = 0$ ) but at  $y = 0.185m$ . This way the tubular junction between the wing and the fuselage body can be horizontal, thus providing more stiffness and strength. The final step for finalizing the aerodynamic design of the wing was to conduct full CFDs with the definitive design in order to gather all possible aero data at different angles of attack and velocities (Fig. 5). The most relevant results are listed in Table 2.

The data gathered was in line with what was expected and aerodynamic performance was deemed acceptable, so the chosen wing was considered final.

## Flap

In deciding how to design the moving surfaces there were two main philosophies we could follow: we could either go for a flaperon or choose to have two separate surfaces, one to work as a flap and the other to function as an aileron, on each semi wing.

Since our experience with flaperons was limited and we didn't want to risk creating a single surface that could eventually prove ineffective at working both as an aileron and a flap, we opted for the traditional configuration. Another reason for this choice was that the competition rules allow multiple radio modes when piloting, so in case of necessity we could still trim the outer ailerons with positive deflection to help the flaps if the latter alone aren't enough.

As for the flap type, we opted for a plain flap as it is the most straight-forward to design, test and build. Also its kinematics are the easiest to fit inside the thin and small wing of the plane.

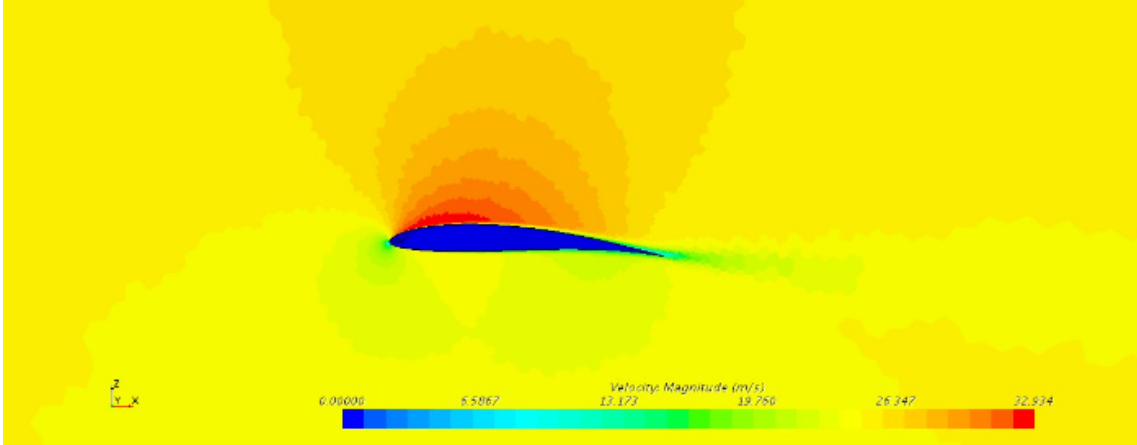


Figure 5: Side-view of the wing,  $v = 25 \text{ m/s}$ ,  $\alpha = 0^\circ$

Preliminary data was collected using XFLR5 in the 2D direct foil analysis tool, while subsequent 3D CFD simulations were carried out to decide the spanwise dimension of the moving surface and gather more precise data on performance gains.

The main takeaways were as follows:

- Optimal deflection angle range:  $\delta = 7^\circ - 13^\circ$ ;
- Optimal angle of attack for maximum lift gain:  $\alpha = 8^\circ - 10^\circ$ .

The final geometry of the flap was thus decided as follows:

- Flap chord:  $c_{flap} = 25\% c_{wing}$ ;
- Flap spanwise extension: from dihedral to 60% of wingspan.

All simulations were run at the expected takeoff speed of  $v = 13 \text{ m/s}$  and angles of attack ranging from  $\alpha = 6^\circ$  to  $\alpha = 13^\circ$  with  $1^\circ$  increments.

## Winglets

The design and simulation of winglets was conducted in order to evaluate whether it was possible to harvest some more efficiency out of the airplane, once all other design aspects had already been cemented.

The design we opted for is one of the simplest: two trapezoidal winglets with root chords equal to the wing's chord, protruding vertically from each wingtip (Fig. 6). Since the winglets are vertical, we decided to use a symmetrical airfoil in order to reduce any additional induced drag. The profile of choice was the S9027 since it offers good efficiency at a neutral angle of attack.

Based on previous experience and similar configurations, we decided to simulate two different models in both takeoff and cruise configurations using CFD with the following parameters:

- Takeoff configuration:  $v_{TO} = 13 \text{ m/s}$ ,  $\alpha = 8^\circ$ ;

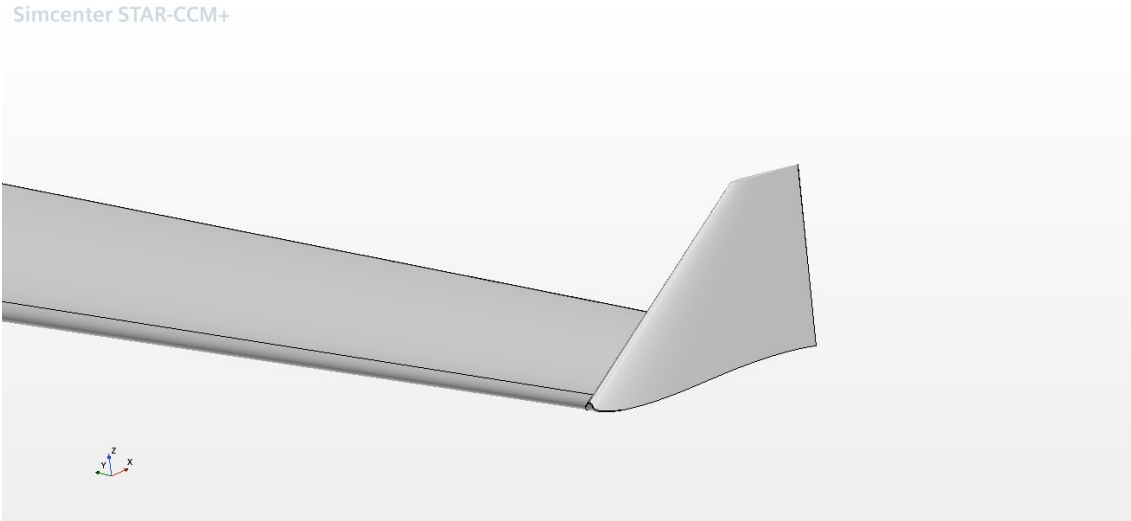


Figure 6: Winglet design

	Tip chord	Root chord	Height	% Efficiency gain takeoff	% Efficiency gain cruise
Winglet 1	30 mm	102 mm	60 mm	1.09%	0.26%
Winglet 2	30 mm	102 mm	80 mm	1.31%	-0.20%

Table 3: Winglets geometries and simulations results.

- Cruise configuration:  $v_{cruise} = 25 \text{ m/s}$ ,  $\alpha = 0^\circ$ ;
- Turbulence model:  $k - \Omega$ ;
- Transition model:  $N/A$

The models geometries and simulations results are listed in Table 3.

Overall, it seems that a taller winglet helps more during takeoff and at high angles of attack but can be detrimental during the cruise phase, therefore for the final geometry we decided to opt for a middle ground between the two models tested. The definitive winglet has the following dimensions:

- Airfoil:  $S9027$ ;
- Tip chord: 30 mm;
- Root chord: 102 mm;
- Height: 70 mm.

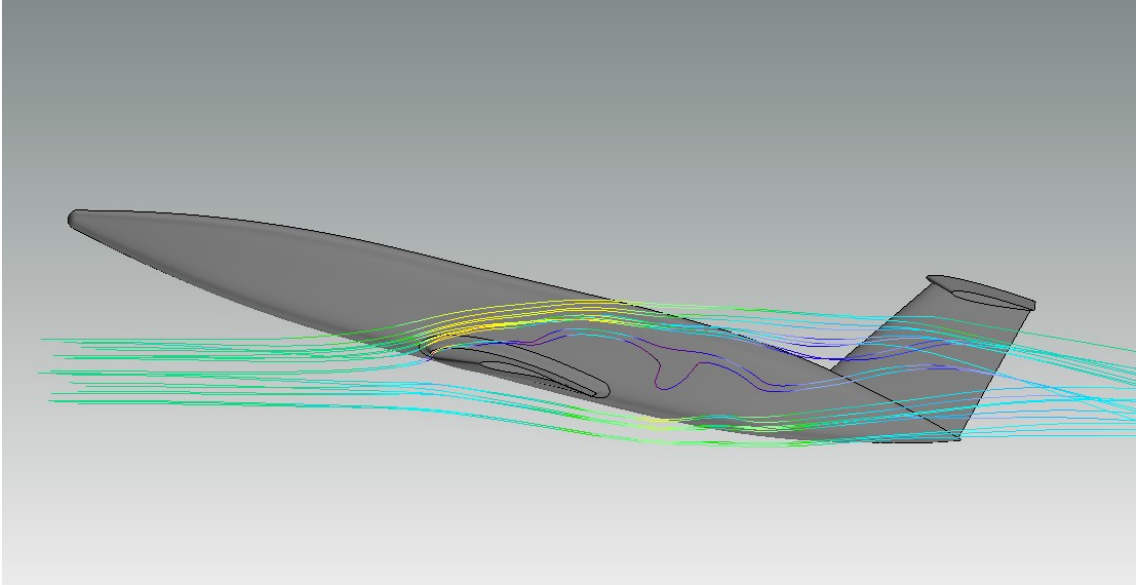


Figure 7: Side-view of the plane,  $v = 25 \text{ m/s}$ ,  $\alpha = 14^\circ$

## Full model simulations

The main objective of a full model simulation is to assess that the whole plane's aerodynamic behavior is in line with what is expected and with the results that have been obtained by previous simulations on single elements or subsystems.

In our case, given the computational expense of a full scale CFD, the aircraft was simulated only at the expected cruise speed of  $25 \text{ m/s}$  and at three different angles of attack:  $0^\circ$ ,  $8^\circ$  and  $14^\circ$ . All simulations were carried out with the  $k - \Omega$  turbulence model and both with no transition model and with the  $\gamma - transition$  model.

The following conclusions were drawn:

- The decrease in performance from the isolated wing to the full airplane is not negligible, but the lift generated at  $\alpha = 0^\circ$  is still sufficient for leveled flight;
- The fuselage, at  $\alpha = 8^\circ$ , contributes much more than expected to the generation of lift;
- At  $\alpha = 8^\circ$  the flow is still attached with no major wake or instability phenomena;
- At  $\alpha = 14^\circ$  the flow over the main wing separates, but the wake does not interfere with the horizontal stabilizer (Fig. 7);
- Due to separation and flow instability, even with no transition model, at  $\alpha = 14^\circ$  the convergence is not optimal;
- The  $\gamma - transition$  simulations do not provide reliable enough results, due to the mesh not being dense enough.

Overall the design of the plane was validated and the results were in line with what was expected.

# Structural design

## Fuselage

For the design process of the fuselage we took as inputs the external shape already defined by the Aerodynamics design, the number of payload bags and their position. Basing on such data we decided that payload bags and electronics should be loaded from above, so we cut the top part of the geometry of the fuselage and opted to compensate for the reduced torsional stiffness with some wooden ribs. This concept was enough to start building a FEM model of the structure, depicted in figure 8.

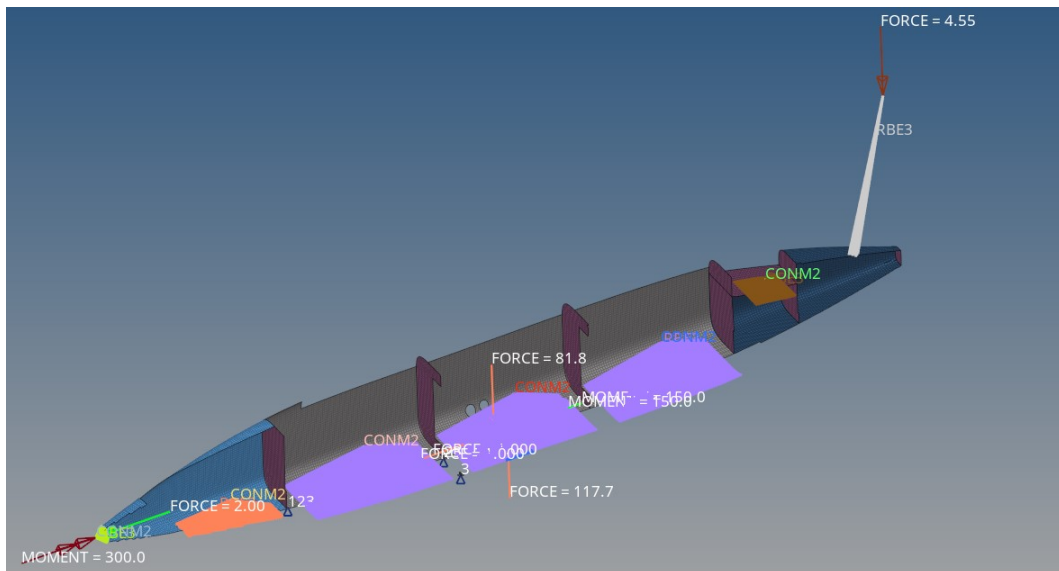


Figure 8: Section of the fuselage model: wooden ribs in violet, load case CRUISE

Loads were applied relying on some estimations performed by Flight Mechanics, who evaluated weights, lift, drag, torques and thrust in 4 different contingencies:

- **STATIC LOAD TEST:** the preliminary Empty Weight acts as a gravity load distributed along all elements, while concentrated masses simulate the weight of payload bags and other components like the electronics.
- **CRUISE:** Forces and moments representative of the loads acting during cruise.
- **TURN:** Simulation of a worst-case unbalanced turn.

- MAX LIFT: Lift and drag acting in CRUISE are multiplied by 3, in order to simulate a maneuver with a contingency factor  $n = 2$  including a 1.5 safety factor.

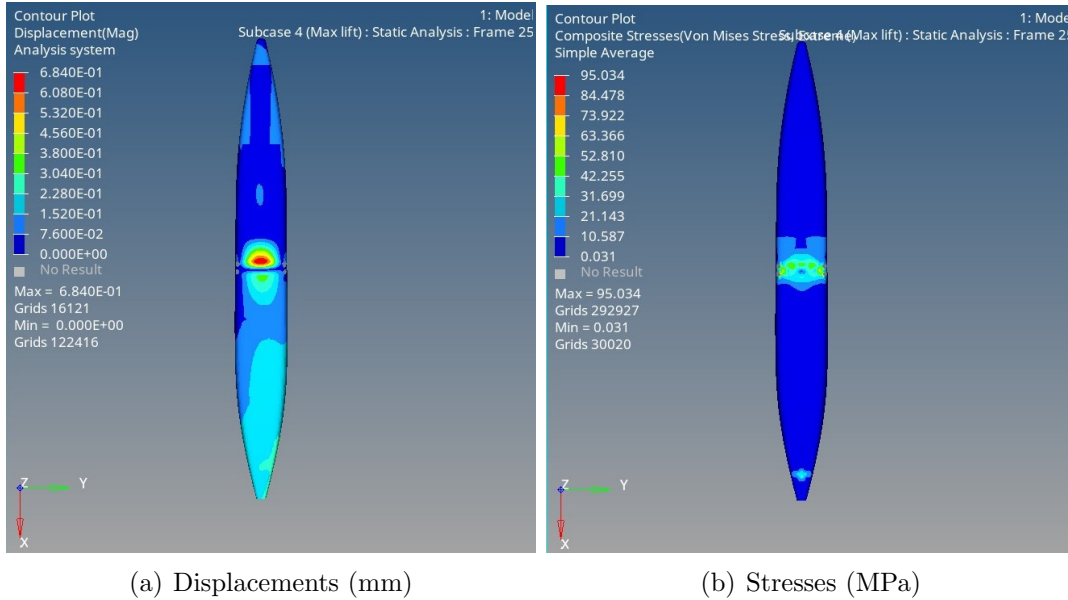


Figure 9: Results for MAX LIFT load case

Except for the STATIC LOAD TEST subcase, the model was constrained only by means of INERTIA RELIEF.

Combining an optimization-based FEM approach and hands-on feedback in terms of manufacturability, we chose a stacking solution featuring a sandwich structure with a Rohacell 51A core and 160 gsm twill carbon fabric faces. Simulations showed that the goal of ensuring high stiffness could be achieved with just one layer of fabric per sandwich face (fig. 9), whilst leaving a large safety margin in terms of resistance. For the sake of simplicity and weight reduction, we retained only 3 out of the 5 wooden ribs. Further studies are ongoing to assess whether we can reduce the weight of the fuselage without compromising too much the stiffness.

## Wing

For the project of the wings we decided to fully integrate stringers and spar caps inside the wing skin, while keeping spar webs in 2 separated elements. In order to implement this concept and achieve the desired properties, we designed a sandwich structure where the layer stacking, from the outside to the inside of the component, is the following one:

- Carboweave (20 gsm): non-woven fabric placed on the whole wing wetted surface mainly in order to obtain torsional stiffness, whilst also collaborating to the flexural stiffness.

- Unidirectional carbon fiber (80 gsm): two narrow layers placed at the third of the local chord, matching the two spar webs. They introduce the most part of the necessary flexural stiffness required during the static ground test, as well as during cruise in order to avoid excessive displacements.
- Rohacell 51A: used as the sandwich core, it introduces shear stiffness and moves the UD layers outwards so that flexural stiffness is maximized.

Each layer, except for the core, is mirrored in the thickness direction, resulting in a symmetrical sandwich. The same stacking applies both for the upper and lower surface of the wing. The rest of the wing structure is made up of balsa ribs and spar webs, which hold the shape of the skin and introduce shear stiffness. In addition, three ribs made of poplar plywood located near the wing root allow the connection with the fuselage.

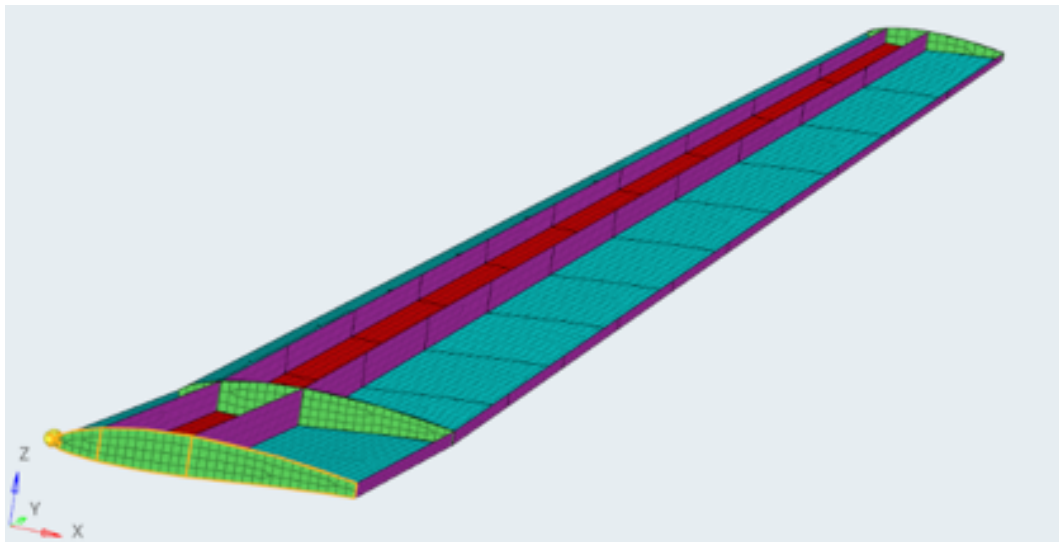


Figure 10: Internal structure used for preliminary studies

The structure was simulated in the worst case scenario of the static ground test, also accounting for a fairly large safety factor in order to consider any imperfection introduced during the construction phase. Displacement results in figure 11 confirm that the configuration chosen is appropriate.

## Tail

The tail assembly is made up of three main components: supports, junction tubes and a vertical fin. The connection with the fuselage is guaranteed by the supports, two components glued to the upper and lower fuselage shell hosting holes for the passage of the tubes, which represent the junction element with the drift. These supports are made of poplar plywood. The junction is composed of two carbon fibre tubes: the main one is placed at the forward third of the fin's chord and has a diameter of 10 *mm*; the secondary tube has a diameter of 8 *mm* and is placed in

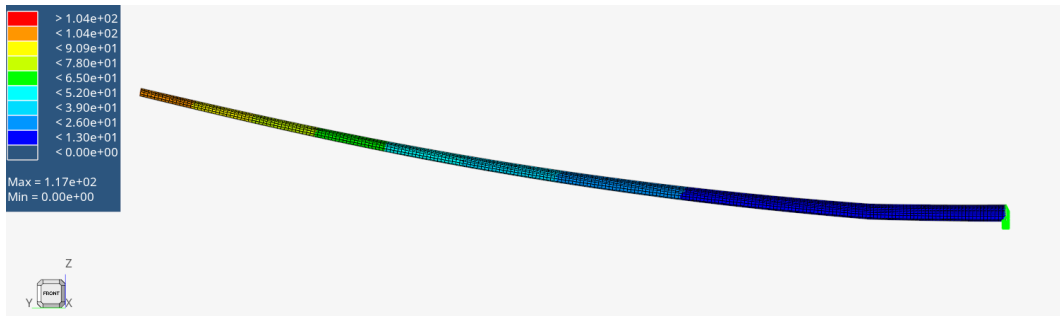


Figure 11: Wing displacement under static testing

front of the previous one blocking the fin's rotation. The main and secondary tube thicknesses are respectively  $1\text{ mm}$  and  $1.5\text{ mm}$ , and they both are COTS component built with the wrapping technique. The tubes are inserted into the polystyrene core of the centreboard on one side and glued with polyurethane glue, while on the other side they are connected to the fuselage through a poplar shim and secured with screws. The centreboard is made of polystyrene wrapped with a 20 gsm Carboweave ply. To increase the rigidity of the structure, some strips of UD fabric are added: one along the upper edge, the second along the lower edge and the third in the same direction of the tubes. This composition is optimal to guarantee the greatest possible stability of the structure during flight. Figure 12 shows the final geometry of the tail, comprising 2 pockets for servo installation.

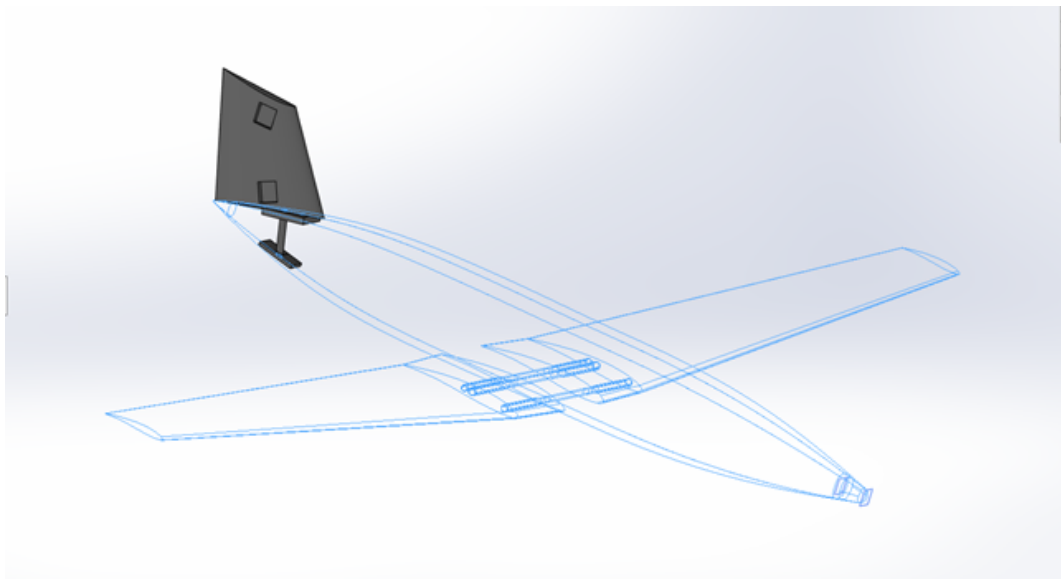


Figure 12: CAD Tail

The structural analyses carried out contemplate a simulation in static conditions, where we distribute the aerodynamic resistance (drag) on the leading edge of the fin and consider the distribution of pressure due to yawing. In the FEM model the last part of chord is deliberately deleted, as it will constitute a mobile part

necessary only for directional control, irrelevant for structure stiffness. By imposing interlocking constraints on the walls of the supports, fixed to the fuselage, and bonding constraints between tubes/supports and tubes/fin, we obtained the results shown in figure 13.

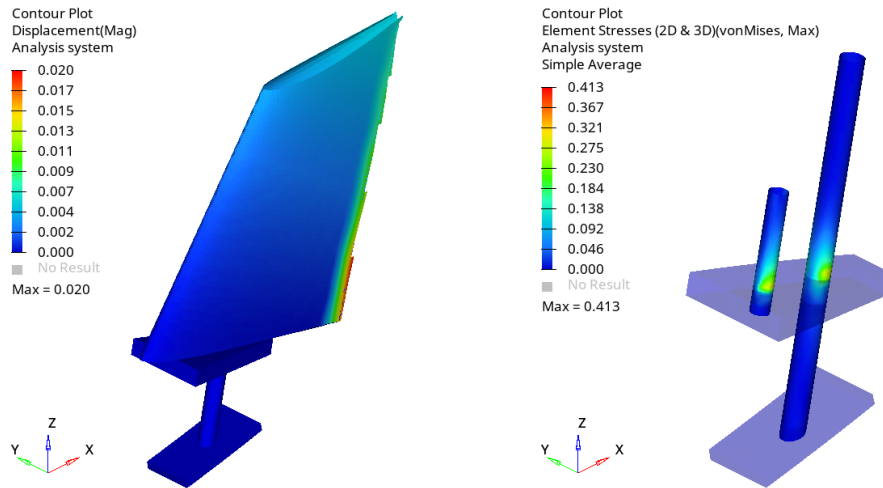


Figure 13: Displacement Tail SX Stresses on the tubes DX

For the loading condition studied, the results show a satisfactory behaviour of both the joint and the fin, well within material and displacement limits.

## Landing Gear

As for the landing gear, we chose to design a single-track tapered component in composite material connected to the wheel by a hub. In a preliminary way we determined its overall dimensions and positioning, taking as inputs:

- Propeller and wheel diameters
- Estimated CG location
- Seating angle during takeoff
- Some additional height in order to get extra propeller/ground clearance and account for elasticity during touchdown

With such basis, the geometry of the single track was modeled with a base coplanar to the bottom surface of the fuselage, so that the largest possible contact surface is guaranteed. The connection between them is realized with removable threaded parts. The final geometry (fig. 14) is characterized by connected shapes both to reduce stress intensification and for feasibility of the manufacturing and construction process.



Figure 14: CAD landing gear

Taking advantage of the stiffness properties of composite materials, we designed a sandwich structure with a layup as follows:

- Biaxial 110 gsm carbon fabric, placed with a  $\pm 45^\circ$  orientation with respect to the component's front/rear symmetry plane.
- Airex C7055 as the core, to maximize stiffness.
- A symmetric layer of biaxial carbon fabric, so as to get a balanced laminate.

The hub is a 4 mm-diameter cylinder in HDPE, which represents the least stiff element and therefore deforms the most, acting as a mechanical fuse during dynamic loading. The analyses performed were:

- Transient analysis: we applied a concentrated load in the hub centreline, which acts following an assumed intensity curve. This starts at 0, then reaches a maximum due to the impact on the ground and finally stabilizes at the value of static loading, represented by the aircraft MTOW. Everything was corrected with an appropriate factor of safety.
- Modal analysis: we studied the first 15 modes of the structure to simulate a fair number of possible configurations assumed by the same under transient conditions.

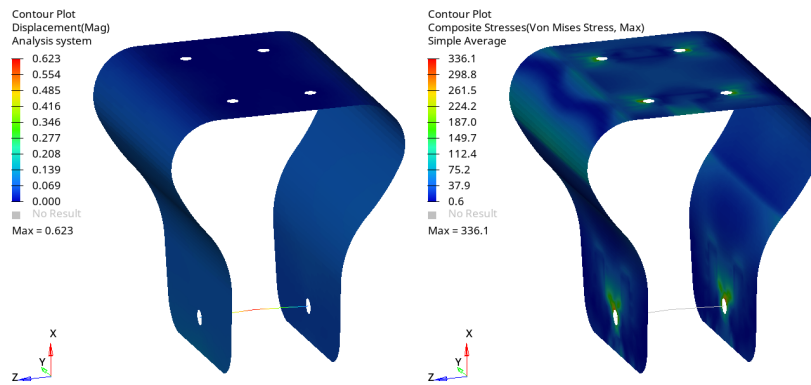


Figure 15: Landing gear displacement SX - Stresses DX

# Manufacturing

## Moulds

One of the techniques used for the construction of the aircraft was to create a mould in Extruded Polystyrene (XPS) using a numerically-controlled milling machine (CNC) in order to get the most accurate shape for the subsequent lamination process. The moulds we produced could have different shapes:

- Negative: a footprint-like mould (fig. 16) where the laminate thickness grows towards the inside of the component. This technique was used for the fuselage and wings.
- Positive: the opposite of above, with a growing direction towards the exterior of the mould. We adopted this method for the landing gear and for tail surfaces, with the peculiarity that for the latter the mould was eventually embedded inside the components.

After having learned independently how to use the machine, we experienced some problems with the joining of thin XPS panels, with their low stiffness and resistance and above all with the removal of components after lamination without damaging the mould. By fine-tuning our lamination process we effectively solved some of these problems, finally obtaining an adequate surface finish.

## Lamination

We applied different lamination techniques for building the aircraft, each one being an adaptation of the classic hand lay-up combined with vacuum bagging and atmospheric curing based on dry fabrics.

With negative moulds and in particular for the fuselage, a crucial aspect was how to pre-form the sandwich core without damaging the mould itself or introducing weak points. Also, given that Rohacell is a closed-cell foam, there was no chance for excess resin to flow towards the absorber during the co-curing process. We addressed this issue by carefully measuring how much resin we poured for each ply, so that excess was avoided and there was enough material to impregnate the fabric and to bond it with the core.

The process for lamination on positive moulds suffered from similar problems, while easing other aspects like the pre-forming of sandwich cores. The component which proved the most difficult to build with such process was the landing gear, because of



Figure 16: CNC working on the fuselage mould

its dimensions and shape. In fact, the fabrics we originally chose for its construction showed too much spring-out during lamination, resulting in a poor adherence with the core and an even worse geometric shape after de-moulding. Since modifying the process could have resulted in introducing additional difficulties, we chose instead to change materials, privileging fabrics over unidirectionals.

For both techniques, we noticed that defects were always concentrated towards the boundaries (mould edges) or near the locations where curvature was the narrowest (wing leading edge, fuselage nose and tail). We eventually improved the finishing in such areas either by modifying the moulds introducing some extra surface, or by hand after the lamination adding a cover patch where it was needed.

# Payload Prediction

In order to estimate the maximum payload that the aircraft can carry in the different atmospheric conditions, we developed a MATLAB script. The script, for every possible combination of air density and airplane mass, calculates the takeoff velocities and distances. Then, considering the regulation limits on takeoff distances, it suggests for each air density the maximum airplane mass, and thus payload, that allows a takeoff in less than 40m or 60m.

As an output, the script generates the dashed curves in fig. 17, which of course are not linear but show different “steps”, because the payload can only be modified in steps equal to the mass of blood bags. Please note that in the graph, the blue curves refer to takeoff in less than 40m, while the red curves refer to a takeoff distance below 60m.

The linear interpolation of such curves yields the following expressions for the predicted payload as a function of the air density:

- Take-off run below 60 meters:  $m = 0.9463 \cdot \rho + 0.8541$
- Take-off run below 40 meters:  $m = 1.0293 \cdot \rho + 0.4048$

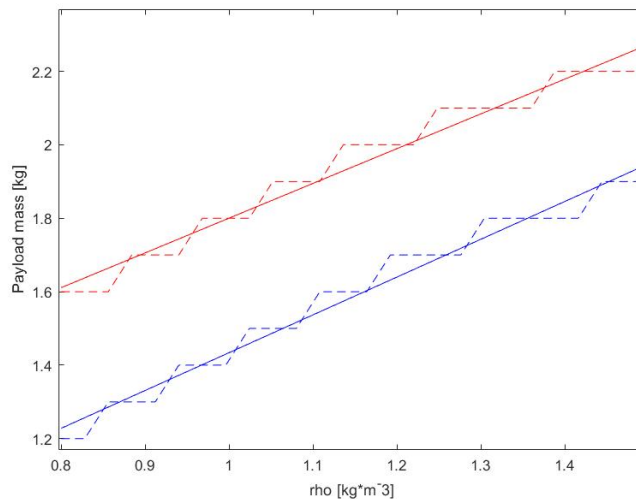


Figure 17: Payload mass - Air density curve resulting from takeoff distance estimation

# Outlook

The first manufacturing iteration of Ichor is reaching its end: we have completed most of the components, and we are in the process of manufacturing the interfaces between them. By building a first prototype, different from the final version, we are practising the construction techniques and verifying what works and what doesn't. As it stands now, everything has already been manufactured with the final methods and materials with the exception of the wing: instead of going directly with carbon fiber, we used fiberglass for the outside skin. This will still provide enough strength to test fly the plane, while being cheaper and easier to build.

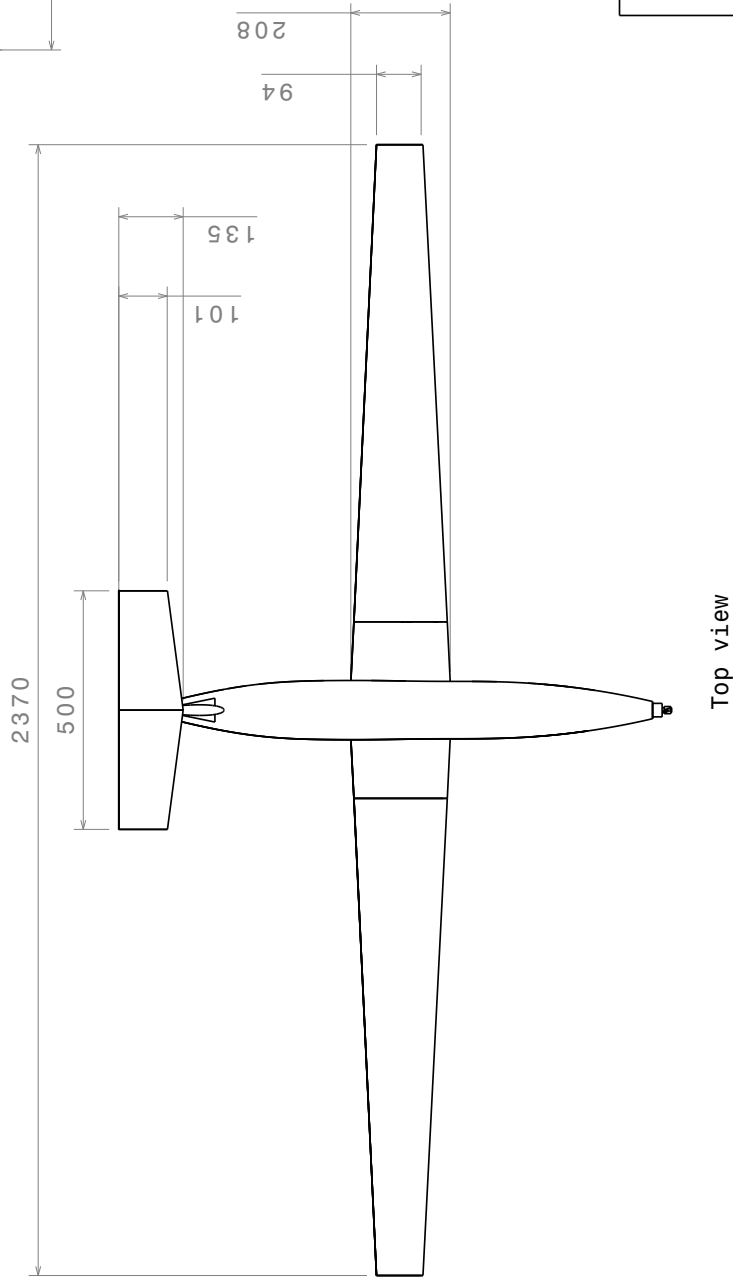
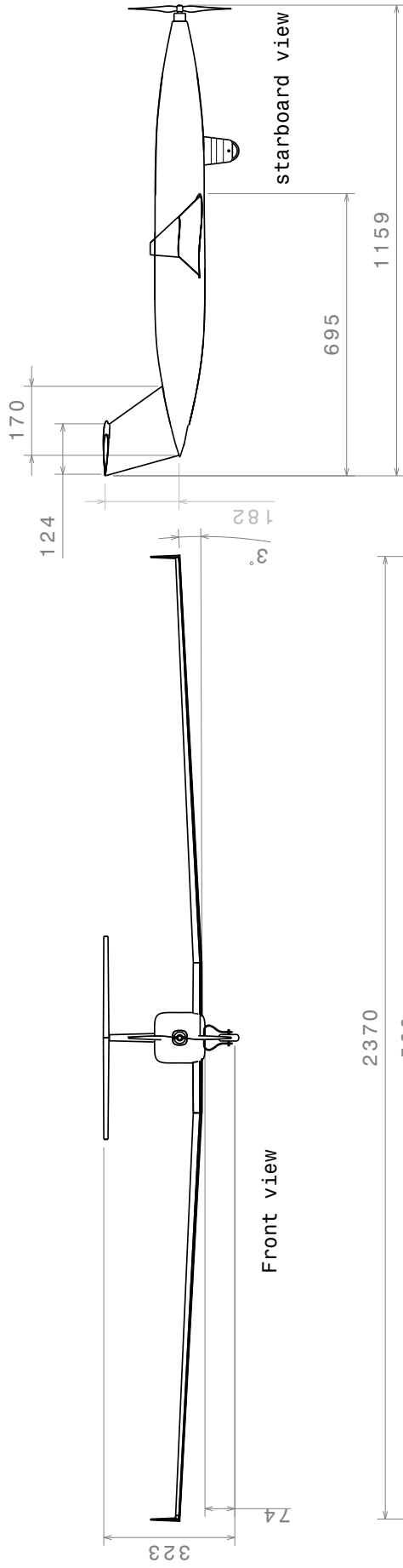
As previously stated, we are having some difficulties with the manufacturing of the landing gear, and its design might change in the future. We also have to verify that the single-wheel approach is usable at takeoff, and that the risk of damage at takeoff doesn't surpass the advantages of creating less drag.

During our test flights we will verify the performance of the plane by comparing it to our payload prediction, and train our pilots. Additionally we will test our loading and unloading procedure as well as the assembly and disassembly of the build.

# Drawings

The drawings that follow provide a detailed summary of the geometry of ICHOR, as well as some useful insights about equipment positioning, joints and much more. In order of apparition, as per the applicable regulation, we have included:

- A 3-view European projection featuring front, top and starboard views
- A port isometric view
- Locations of cargo bay, batteries, motor, RC receiver and GPS measuring equipment
- Servo locations for flaps and ailerons, wing internal reinforcements' architecture and joint details for the tail unit



Scale 1:10

wing area	0,379 m <sup>2</sup>
horizontal stabilizer area	0,059 m <sup>2</sup>
fuselage volume	0,011 m <sup>3</sup>
tail volume	0,527
MAC	0,167 m
aspect ratio	14,825
wing airfoil	AH 79-100 A



Team 22 ICARUS Polito  
Polytechnic University of Torino

all the measures are in mm unless otherwise indicated

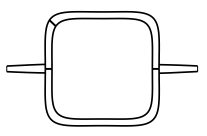
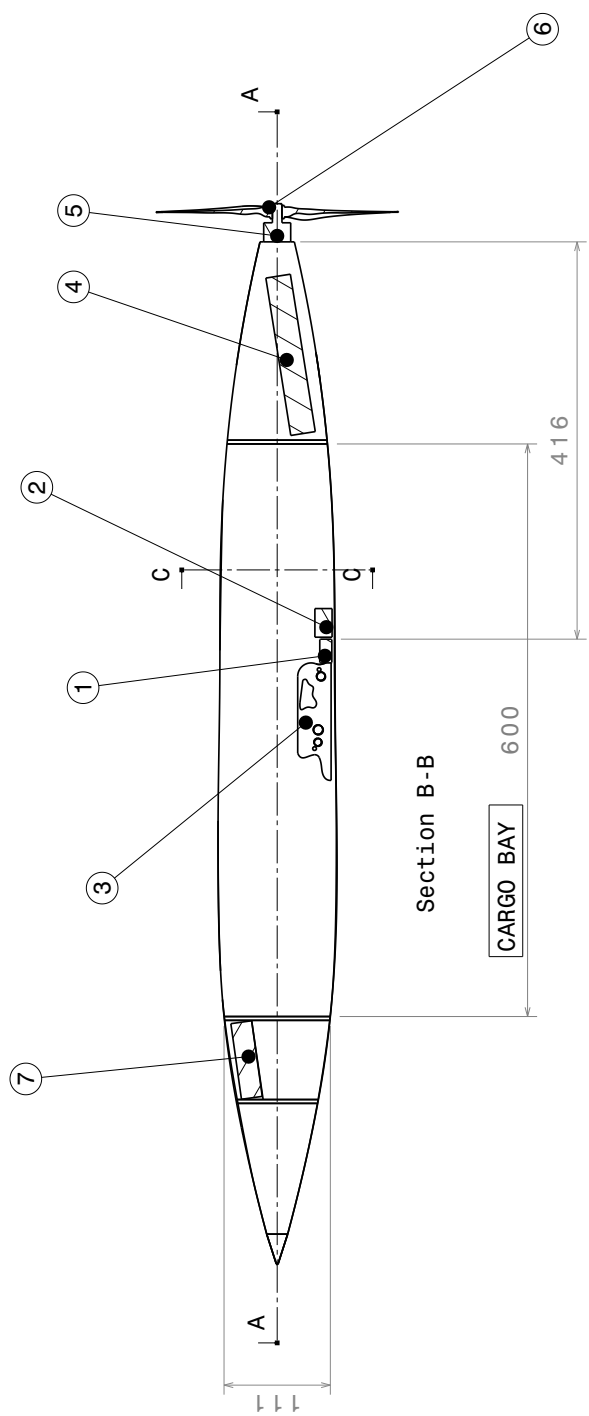


Isometric view  
Scale: 1:5



Team 22 ICARUS Polito  
Polytechnic University of Torino

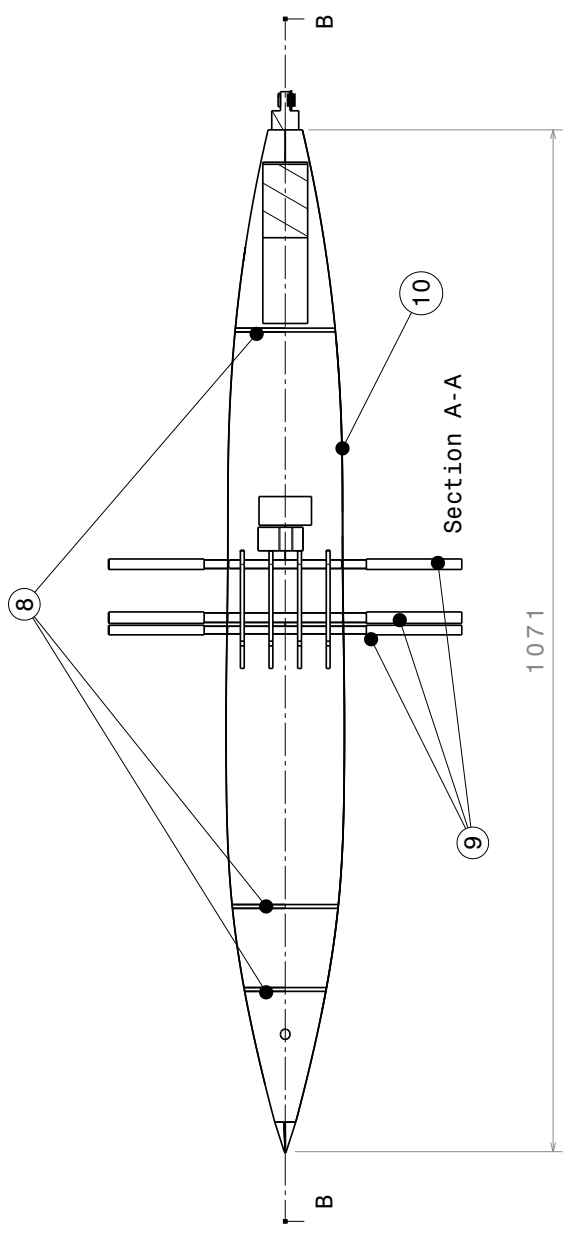
Cargo bay section



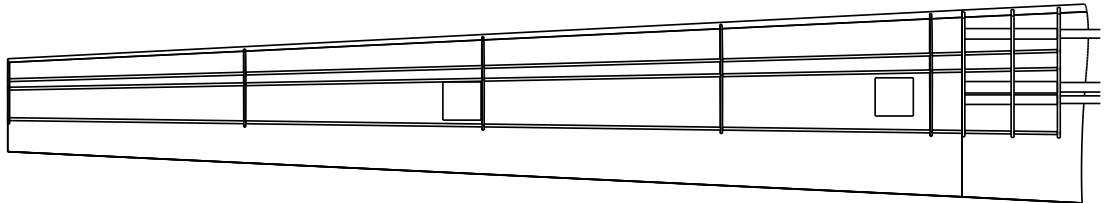
Section C-C

Scale 1:5

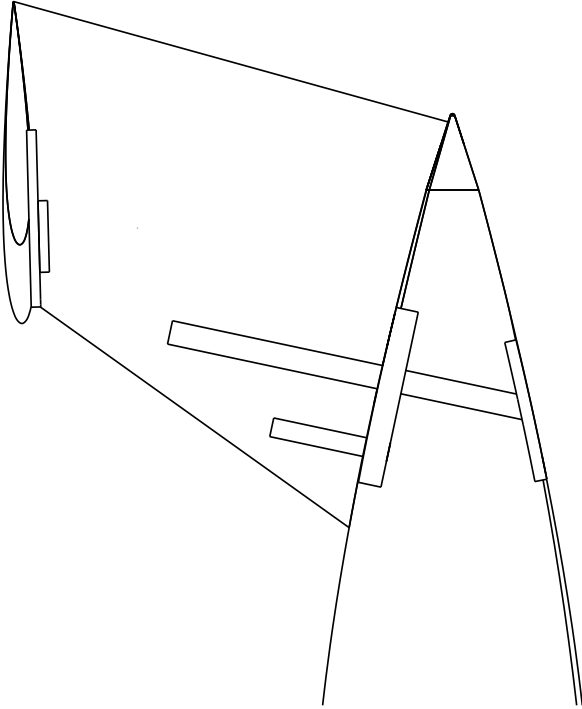
ITEM	NAME
01	receiver (RC)
02	RC battery
03	tubes support
04	engine battery
05	engine
06	propeller
07	GPS
08	ribs
09	tubes
10	fuselage



Team 22 ICARUS Polito  
Polytechnic University of Torino



Left wing particular, position of the servos  
Scale: 1:5



Particular of fuselage-vertical stabilizer junction  
Scale: 1:2



Team 22 ICARUS Polito  
Polytechnic University of Torino